Pharmacokinetics, tissue distribution, effect on proliferation inhibition and apoptosis of hepatic stellate cells and molecular mechanism of Suc-GTS- lip which is glycyrrhetinic acid derivative receptor-mediated liver- targeting liposome

Tao Lin
Beijing University of Chinese Medicine
Xiuli Wang (Lnwangxiuli@163.com)
Beijing University of Chinese Medicine
Huida Guan
Beijing University of Chinese Medicine
Jiahao Lin
Beijing University of Chinese Medicine
Geng Li
Chinese Academy of Medical Sciences & Peking Union Medical College
Yurong Wang
Beijing University of Chinese Medicine

Research Article

Keywords: 18-GA-Suc, compound liposomes, pharmacokinetics, tissue distribution, in vivo imaging, active liver targeting.

Posted Date: April 12th, 2022

DOI: https://doi.org/10.21203/rs.3.rs-1521908/v1

Abstract

Objective To investigate the liver targeting effect of salvianolic acid B (Sal B)-tanshinone IIA (TSN)-glycyrrhetinic acid (GA) liposomes (GTS-lip) with the incorporation of 3-succinic-30-stearyl glycyrrhetinic acid (18-GA-Suc)and To confirm the efficacy of it in treating hepatic fibrosis at the cellular level.

Method 18-GA-Suc was inserted into GTS-lip to prepare GA-derived receptor-mediated active targeting liposomes (Suc-GTS-lip). Compared the pharmacokinetics and tissue distribution of Suc-GTS-lip with GTS-lip.The proliferative inhibition rate of hepatic stellate cell (HSC) affected by Suc-GTS-lip was determinded by MTT assay. The apoptosis rate of HSC was measured with Annexin V-FITC / PI method using flow cytometry. The expression levels of MMP-1, TIMP- 1, TIMP-2, Collagen-Ⅰ and Collagen-Ⅲ mRNA in HSC were determined by RT-PCR.

Result The results of the pharmacokinetic study showed that incorporation of ligands changed the bioavailability of the three liposomal drugs in mice. Tissue distribution results showed that the AUC and Cmax of Sal B were increased in Suc-GTS-lip compared with GTS-lip. The liver targeting effect of Sal B, which was entrapped in the aqueous phase, was achieved with the help of ligands. The in vivo imaging study showed that the modified liposomes tended to accumulate in the liver, with the liver fluorescence intensity reaching its peak at 30 min. The MTT test results showed that Suc-GTS-lip could significantly inhibit the proliferation of HSC and high, medium, low dose groups of Suc-GTS-lip induced apoptosis rates of HSC, which were 75.23 ± 2.56%, 27.60 ± 0.95%, 20.77 ± 3.97%.The RT-PCR results showed that, compared with the blank control group, the Suc-GTS-lip could increase matrix metalloproteinases (MMP-1), high-dose, medium-dose group($P < 0.001$), low-dose group($P < 0.01$);decrease tissue inhibitor of matrix metalloproteinases (TIMP-1 and TIMP-2), high-dose group($P < 0.001$), medium-dose group($P < 0.01$); and lessen synthesis of collagen-Ⅰand collagen-Ⅲ, high-dose, medium-dose group($P < 0.001$), low-dose group($P < 0.05$), suggesting that Suc-GTS-lip may induce the apoptosis of HSC from many ways.

Conclusion Suc-GTS-lip could therefore promote the -stabilities of the drugs and enhance their liver targeting ability.The efficacy of Suc-GTS-lip in the treatment of hepatic fibrosis was confirmed from the cellular level, which provided a basis for the animal efficacy in vivo.

1 Introduction

Hepatic fibrosis is a common pathological feature of various chronic liver diseases. It is caused by excessive synthesis and deposition of collagen in liver extracellular matrix (extracellulr matrix, ECM) (Deng et al.2021).As the intermediate link between chronic liver disease and cirrhosis, liver fibrosis is the wound healing after chronic liver injury. Blocking and reversing liver fibrosis is the key target in chronic liver disease treatment. Myoblast fibroblasts are the main source of extracellular mechanical matrix and hepatic stellate cells can be transformed into myoblasts under injury stimulation.(Ye et al.2021)

Salvia miltiorrhiza and glycyrrhizin are commonly used for the clinical treatment of hepatic fibrosis, and the combination of the two drugs can play a synergistic role in promoting blood circulation and removing

blood stasis.

Salvia miltiorrhiza (Hu et al.1999), of which its active ingredients are Sal B and TSN, can inhibit liver fibrosis formation on the cellular, molecular and genetic levels, and it also plays a role in a number of stages of hepatic fibrosis pathogenesis. Furthermore, it has been proven (Cui et al.2003; Mao et al.2003;Wang et al.2006; Kan et al.2019) that Sal B and TSN have definite effects on liver fibrosis. Glycyrrhetinic acid (GA) is the active metabolite of glycyrrhizin, which is the major pharmacologically active component of *Glycyrrhiza uralensis*. GA is non-toxic and cheap, its effectiveness on liver fibrosis has been demonstrated (Zhu et al.2017). A pharmacological study (Wang et al.1997) showed that GA can enhance liver detoxification capacity, reduce inflammatory response in liver cells, alleviate damage on liver cells from a variety of pathogenic factors and reduce the degree of liver fibrosis in rats. Additionally, GA also has strong liver cell targeting, which makes it a goodcandidate for studies involving novel liver-targeted drugs (Tian et al.2006).

The three components Sal B, TSN and GA are often used together in the clinical treatment of hepatitis in China. All three drugs have been proven to treat hepatic fibrosis at various areas of the body, and at the cellular and gene levels, but the mechanisms and targets of action are not the same. The effect of the drugs combined into one formulation is better than that of the individual compounds, and this can exert a good synergistic effect while greatly reducing the dosage needed. Moreover, GA has been deemed a good liver target both in vivo and in vitro, and has been widely used as a ligand for target therapy of liver disease. Therefore, considering that the three drug ingredients have different polarities, we have chosen liposomes which can simultaneously encapsulate different polarity drugs.

In the early twentieth century, Paul Ehrlich first proposed the concept of targeted drug delivery (Yang et al.2006). Liver targeting drug delivery systems can transport drugs to the liver efficiently, reduce their systemic distribution, decrease the dosage and frequency of administration, and reduce side effects. In recent years, researchers (Fan et al.2007) found that there were many specific receptors on the surface of hepatocytes, among them the GA acceptor. In the 1990s, Ishida, et al. confirmed that there were specific binding sites of glycyrrhizin on the surface of rat liver cells, and there is rapid liver uptake after intravenous injection of GA (Ishida et al.1989). Soon after, Mao et al. successfully incorporated GA derivatives into liposomes to produce hepatocyte-targeted liposomes surface- modified by GA (Mao et al.2003). Wu et al. further compared the tissue distribution in mice between norcantharidin liposomes and norcantharidin liposomes modified by GA stearyl ester-galactosidase, and the result showed that the liver targeting coefficient increased to 5.21 after modification, indicating the superior liver targeting of the modified liposomes (Wu et al.2008). These GA-modified liposomes were thereafter received by US pharmaceutical patents (Yuan et al.2015). In this study, liposomes were modified by GA, which played an active liver targeting role and allowed the drug to be rapidly ingested by the liver.

In this paper, the liposome (Suc-GTS-lip) was prepared, encapsulating Sal B, TSN and GA, and 18-Suc-GA was inserted into phospholipid bilayer as a mediator of hepatocyte targeting. To further prove the liver targeting of Suc-GTS-lip, an *in vivo* imaging method was used to trace the drug in mice. Wavelengths of

excitation and emission of near-infrared dye DiR iodide are 748 nm and 780 nm, respectively, chosen so as to avoid the influence of spontaneous fluorescence which can occur with *in vivo* imaging. Moreover,the Suc-GTS-lip tissue distribution experiment has shown that the fat-soluble drug in Suc-GTS-lip does not show good liver targeting, probably because the drug is contained in the outer lipid layer of the liposome and enters the liver. It is metabolized soon, so the measurement results are relatively low. Therefore, this experiment selects the fat-soluble fluorescent dye DiR, DiR is not easily metabolized by the liver, and can maintain strong fluorescence intensity within 360min. Thus, in the present study, we track the *in vivo* distribution of Suc-GTS-lip in mice after intravenous injection of DiR-labelled Suc-GTS-lip.

2 Materials And Methods

2.1 .1 Materials and reagents

Sal B, TSN and GA used as liposome raw materials were purchased from Baoji GuoKang Biotechnology Co., Ltd. (Shanxi, China) with the purity >98%. The same reagents used as quantitative analytes and chloromycetin were obtained from National Institutes for Food and Drug Control (Beijing, China). Cholesterol was purchased from Amresco, Inc. (OH, USA). Soybean phospholipid was purchased from Lipoid (Germany). DiR iodide [1,1-dioctadecyl-3,3,3,3-tetramethylindotricarbocyanine iodide] was purchased from Fan Bo Biochemical Co., Ltd. (Beijing, China). Fetal bovine serum was purchased from Gibco Co., Ltd. (USA), DEME liquid medium and PBS buffer were purchased from Corning Co., Ltd. (USA), Trypsin and pancreatin termination solution were gained from Sciencell Co., Ltd. (USA), MTT assay kit was purchased from Tianenze Gene Technology Ltd.Human HSC cell line were provided by the Beijing Wangjing Hospital Pathology department.Urethane was purchased from Sinopharm Chemical Reagent Co., Ltd. (Shanghai, China). Acetonitrile and methanol were HPLC grade and all other reagents were of analytical grade.

2.1 .2 Instruments

Incubator Model BB16UV/BB5060UVCO2 was purchased from Heraeus, The low-speed medical centrifuge Model 40C was from Baiyang centrifuge factory (Anxin, China),The triple purpose thermostatic water tank Model SHH.W21.600 was purchased from Shuli Instrument Co.,Ltd.(Shanghai, China) , The clean bench Model HF safe 1500 was obtained from Lishen Scientific Instrument Co.,Ltd. (Shanghai, China), The low-speed shock meter Model DTY-2000 was purchased from Detianyou Technology Development Co., Ltd.(Beijing, China), The microplate reader Model 680 was from BIO RAD.The electron microscope Model Eclipse TE2000-5 was purchased from Nikon Corporation(Japan),The flow cytometry Model FACSC anto was from BD Corporation(USA).

2.2 18-GA-Suc synthesis process

The first step: weigh 2.7g of stearyl alcohol in 20mL of anhydrous dichloromethane, add 1-ethyl-(3-dimethylaminopropyl) carbodiimide hydrochloride (EDC-I). After stirring at 80 ° C with constant temperature, 4.7 g of GA was added and stirring was continued. The reaction solution was concentrated,

and separated by silica gel column chromatography, eluting with a solvent gradient of methanol-dichloromethane, and recrystallized to get a white solid, which was confirmed to be intermediate 18-GA by NMR and carbon structure.

Second step: 695 mg of 18-GA was weighed and dissolved in 20 mL of anhydrous dimethylformamide (DMF) solution, 150 mg of succinic anhydride and an appropriate amount of EDC-I were added, and the mixture was stirred under vacuum at 100 °C. The residue was diluted and stirred at room temperature and extracted with dichloromethane. The combined organic layer was washed with brine, dried over sodium sulfate, and then evaporated. The spectrum and carbon spectrum structure were confirmed to be 18-GA-Suc.

2.3 Preparation and characterization of GTS-lip and Suc-GTS-lip

GTS-lip was produced as described previously (Lin et al., 2014) and Suc-GTS-lip was made, with some modification, on the basis of this previous method. Two hydrophobic ingredients and the ligand, namely, GA, TSN and 18-GA-Suc, were embedded in phospholipid bilayers by the thin film-ultrasound method to form Suc-GT-lip. The ratio between soy lecithin (SPC) and cholesterol (CH) was 6:1 (w/w), SPC and TSN 30:1 (w/w), and SPC and GA 24:1 (w/w). The hydrophilic ingredient Sal B was dissolved in glycine-HCl buffer with pH 3.32. This solution was then added dropwise into Suc-GT-lip and altogether placed into a water bath at 30 ^{o}C for 30 min to obtain Suc-GTS-lip. The liposome was characterized for particle size, size distribution and entrapment efficiency.

2.4 In vitro release experiments

Three copies of Suc-GTS-lip mixed with GA and TSN were absorbed in parallel. Each 3 mL was placed in 100 mL 0.5% SDS release effluent. 3 mL of release medium was added to the pretreated dialysis bags, and the two ends were tightly immersed in the release of the external liquid. The stirring paddle speed was 100 r·min^{-1}, and the temperature was controlled at 37 °C. One dialysis bag was taken out at 1h, 2h, 4h, 8h, 12h, 18h, 24h, 36h, and an equal amount of isothermal release medium was added. The TSN and GA contents were determined by HPLC, and the cumulative release percentage of the drug was calculated and fitted to the model.

2.5 In vivo pharmacokinetics and tissue distribution study

2.5.1 Animals

5-week-old, 20 ± 2 g male Kunming mice [SCXK (Jing) 2011-0004] were all purchased from SPF Biotechnology Co., Ltd. (Beijing, China). All animal procedures were performed according to animal care protocols approved by the Ethics Committee of Beijing University of Chinese Medicine in accordance with the National Institute of Health Guide for the Care and Use of Laboratory Animals.

2.5.2 Drug administration and sampling

For the pharmacokinetics and tissue distribution study, one hundred mice were randomly distributed into two groups, each containing fifty animals. One group was administered GTS-lip at a dose of 48.25 mg/kg body weight for Sal B, 4.88 mg/kg body weight for TSN and 26.12 mg/kg body weight for GA, while the other group received Suc-GTS-lip by tail intravenous injection at equivalent doses as the GTS-lip group. Mice eyeballs were extracted and blood samples were collected into heparinized Eppendorf tubes and the heart, lungs, liver, spleen, and kidneys were collected at 0.083, 0.17, 0.33, 0.5, 0.75, 1, 1.5, 2, 4, and 6h. Plasma was collected from the blood samples by centrifugation at 15000 rpm for 10 min and stored at -20 ^{o}C. All of the tissue samples were flushed with saline and stored at -20 ^{o}C until further analysis.

2.5.3 Plasma sample treatment

50 μL of formic acid:water (v:v = 1:3) solution and 10 μL chloromycetin internal standard (0.2 mg/mL) were added to 150 μL plasma. Acetonitrile (1 mL) was then added, and the samples were vortexed for 3 min and centrifuged at 15000 rpm for 10 min to precipitate the proteins. The supernatants were transferred to another Eppendorf tube and to the remaining precipitations was added another 1 mL acetonitrile. The supernatants of this double extraction were combined to dry up. The residues were redissolved in 100 μL of methanol, vortexed for 1 min and centrifuged for 10 min at 15000 rpm. Samples were then analyzed by UPLC.

2.5.4 Tissue sample treatment

Tissue samples were thawed, cut into pieces and added into saline for further homogenization. Formic acid:water (v:v = 1:3) solution (70 μL for liver and kidney, 50 μL for spleen, lung and heart) and 10 μL of chloromycetin were added into a certain amount of tissue homogenates (500 μL of liver and kidney, 150 μL of heart and spleen, 250 μL of lung). The extraction and other process were same as above.

2.5.5 UPLC analysis

UPLC analyses of mouse plasma and tissue samples were performed using a Waters ACQUITY UPLC series with binary solvent management system, on-line degasser, automatic sampler and photo-diode array (Waters Co., USA). Chromatography was recorded on an ACQUITY UPLC® BEH C18 reverse-phase column (2.1 mm×50 mm, particle size 1.7 μm) (Waters Co., USA). The injection volume was 1 μL. The mobile phase consisted of a mixture of acetonitrile (solvent A) and 0.5% formic acid in water (solvent B) with gradient elution and was pumped at a flow rate of 0.4 mL/min with 30 °C column oven temperature, and column eluents were monitored by dual-wavelength spectrophotometry (289 nm for Sal B, 265 nm for TSN, 254 nm for GA). The linear gradient elution program was as follows: (1) from 20% A to 25% A in 0-1.5min, (2) from 25% A to 64% A in 1.5-3 min, (3) held at 64% A in 3-5.1 min, (4) from 64% A to 90% A in 5.1-5.8min, (5) from 90% A to 20% A in 5.8-6.0 min.

2.5.6 In vivo imaging and ex vivo imaging of mouse organs

Mice were anesthetized by urethane, and intravenously injected with 0.2 mL Suc-GTS-lip, which was labeled with a lipophilic near-infrared fluorescent dye (DiR-iodide, 10 μg/kg). A small animal *in vivo* imaging device was used obtain fluorescent images at 10, 30, 60, 120, 240, and 360 min after administration, and images were taken at the same exposure intensity and exposure time.

Experimental animals were sacrificed after intravenous administration of GTS-lip and Suc-GTS-lip at 10, 30, 60, 120, 240, and 360 min (n = 3 for each time point), and the heart, liver, spleen, lungs and kidneys were collected.

After removing the blood, the organs were imaged using the small animal fluorescence imager and their exposure intensity and time were normalized.

2.5.7 Pharmacokinetic and tissue distribution data analysis

Pharmacokinetic parameters and tissue distribution of Sal B, TSN and GA were calculated using non-compartmental methods (Winnonlin 5.2, Pharsight, Certara USA, Inc.).

SPSS statistical software version 17.0 (SPSS Inc., USA) was used for statistical data analysis. Student's t-test was used for comparative analysis between two groups of pharmacokinetic parameters. One-way ANOVA was employed to compare data between multiple groups.

2.6 Effect of Suc-GTS-lip on proliferation inhibition and apoptosis of hepatic stellate cells

2.6.1 Cell Culture

Both cell lines were cultured with Dulbecco's Modified Eagle's Media (DMEM) supplemented with 10% fetal bovine serum in a humidified atmosphere of 5% CO2 at 37℃. The medium was replaced with fresh medium every other day until the cells grew to about approximately 80%.Then Suc-GTS-lip were diluted at different concentrations with DMEM.

2.6.2 Grouping and drug administration

HSC cells were divided into two groups. One group was used to study the effect of Suc-GTS-lip on the proliferation inhibition of hepatic stellate cells in different doses, and the other was used to study the effect of Suc-GTS-lip on apoptosis of hepatic stellate cells in different doses.

In the study of the effect of Suc-GTS-lip on the proliferation inhibition of hepatic stellate cells, the groups and the drug loading concentrations of liposomal Suc-GTS-lip were shown in table 1 below. 200μL single cell suspension(1.0 × 105/mL) were plated in 96-well plates and incubated at 37°C and 5% CO2 until the culture plate was covered around 80%,different concentrations of drugs were administered to 7 groups mentioned below. Every group was provided with 6 sane holes and cultured under the same condition.

Table 1 Grouping and dosing of Suc-GTS-lip

Groups	SalB（μM）	TSN（μM）	GA（μM）	18-GA-Suc（μM）
Suc-GTS-lip1	600	80	300	300
Suc-GTS-lip2	300	40	150	150
Suc-GTS-lip3	150	20	75	75
Suc-GTS-lip4	75	10	37.5	37.5
Suc-GTS-lip5	37.5	5	18.75	18.75
Blank-lip	——	——	——	——
Healthy Cells（Control Group）	——	——	——	——

In the study of the effect of Suc-GTS-lip on apoptosis of hepatic stellate cells, the groups and the drug loading concentrations of liposomal Suc-GTS-lip were shown in table 2 below. 2mL single cell suspension(1.0 × 105/mL) were plated in 6-well plates and incubated at 37°C and 5% CO2 until the culture plate was covered around 80%,different concentrations of drugs were administered to 4 groups mentioned below. Every group was provided with 3 same holes and cultured under the same condition.

Table 2 Grouping and dosing of Suc-GTS-lip

Groups	SalB（μM）	TSN（μM）	GA（μM）	18-GA-Suc（μM）
Suc-GTS-lip（High-dose）	300	40	150	150
Suc-GTS-lip（Medium-dose）	150	20	75	75
Suc-GTS-lip（Low-dose）	75	10	37.5	37.5
Healthy Cells（Control Group）	——	——	——	——

2.6.3 MTT Assay

In the study of the effect of Suc-GTS-lip on the proliferation inhibition of hepatic stellate cells, after administration ,the cells were incubated at 37°C and 5% CO2 for 24 and 48 hours. After removing the supernatant we added 100 μL fresh medium and 10 μL solution A (containing MTT component) were added into 96-well plates. After incubation for 4 hours, original medium was removed and 110 μL solution B was added into each well and shaked 10 min by low volatility. Absorbance was detected at 490 nm with the enzyme-linked immunosorbent detector (EIA). The inhibition rate of cell proliferation was calculated according to the following formula, and the A was absorbance.

inhibition rate of cell proliferation=（A_0-A_i）/A_0×100%

Ai indicated the absorbance value which was in the experimental group, and A0 indicated the absorbance value which was in the control group.

2.6.4 Determination of HSC apoptosis rate by Annexin V-FITC/PI method

In the study of the effect of Suc-GTS-lip on apoptosis of hepatic stellate cells, after administration, the cells were incubated at 37°C and 5% CO2 for 24 hours. After removing the supernatant, the HSC cells were monitored the morphology of in each group.

The corresponding loading liposomes (Suc-GTS-lip) were added into the incubator according to the grouping requirements. After 24 hours, the primary culture medium was discarded and the cells were collected by 0.25% trypsin digestion without Ethylene Diamine Tetraacetic Acid (EDTA). 1 mL cells mentioned above were centrifuged for 10 min in 1000 rpm and the supernatant was discarded.Then1 mL pre-chilled PBS was added, the cells were suspended with shaking and centrifuged in 1000 rpm for 10 min and the supernatant was discarded. Repeat the step above two times. And then the cells were resuspended in 200 μL Binding Buffer. Next,10 μL Annexin V-FITC and 10 μL PI were added and mixed and put them in dark room for 15 min.Last, Detect apoptosis rate by flow cytometry within 1 h.

2.6.5 Primer design and RNA electrophoresis separation

Primer design was shown in Table 3.

Table 3 Primer design

Primer name	Primer sequence (5'to3')	Amplification product size (BP)
MMP-1 F	CCTCTGGCTTTCTGGAAGGG	267
MMP-1 R	CCACATCAGGCACTCCACAT	
TIMP-1 F	CTCGTCATCAGGGCCAAGTT	312
TIMP-1R	GTAGGTCTTGGTGAAGCCCC	
TIMP-2 F	TGCACATCACCCTCTGTGAC	
TIMP-2R	TGGACCAGTCGAAACCCTTG	362
Collagen –I F	AGAGGTCGCCCTGGAGC	425
Collagen –I R	GGAGAGCCATCAGCACCTTT	
Collagen –III F	GAGCTGGCTACTTCTCGCTC	285
Collagen –III R	CCTTGACCATTAGGAGGGCG	
Beta-Actin F	TGACGTGGACATCCGCAAAG	185
Beta-Actin R	CTGGAAGGTGGACAGCGAGG	

8 μL RNA was electrophoresis analyzed with 1% agarose gel.

2.6.6 Reverse Transcription

HiFi-MMLV cDNA（Cat#CW0744）was used to reverse transcription. Experimental operation follows the product instructions:

(1) RNA template, primers, 5xRT mix and RNase-free Water were dissolved and placed on ice to spare.

(2) Add and mix 20ul the first part of the reaction system to the tube as follows.

Reagents	20μL Reaction System	Final concentration
Primer mix	2 μL	50 uM
RNA Template	2 μL	10 ng
RNase-Free water	To 15 μL	

(3) Incubate for 5 min at 65℃, then put it into the ice bath immediately for 2 min and centrifuge briefly, last collect the solution.

(4) Continue add the following reagents:

Reagents	20μL Reaction System	Final concentration
RT Mix,5x	4μl	1×
HiFi-MMLV Enzyme Mix	1μl	

(5) Mix and incubate for 40 min at 37℃. After the reaction, keep warm at 70 ℃for 10 minutes.

2.6.7 Reverse Transcription PCR

(1) RT-PCR reaction system:

Reagents	20μL Reaction System
Pcr Mixture (2 ×)	10 μL
The upstream primer (10μM)	1.5 μL
Downstream primer (10μM)	1.2 μL
Template	2 μL
Sterile distilled water	To 20 μL

(2) The reaction system was used to amplified, the experimental operation followed by PCR mixture product instructions. The amplification program was: 95℃ for 10 min, 95℃ for 15 s, 59℃ for 60 s × 30 cycles.

(3) All the amplified products were electrophoretic analyzed by 5ul.

2.6.8 The Statistical Treatment

The relative quantitative analysis of the data was carried out by gray scale analysis with BIOER PCR instrument.

The quantitative gray value is expressed by X + s, and the data are processed by SPSS17.0 statistical software. Two samples were compared by T test, and One-way ANOVA was used among the groups.

3 Results

3.1 Characterization of GTS-lip and Suc-GTS-lip

The entrapment efficiency (EE), drug loading rate (DL), particle size, zeta potential and incorporation ratio of 18-GA-Suc (IR) of GTS-lip and Suc-GTS-lip are shown in Table 4.

Table 4
Physicochemical properties of GTS-lip and Suc-GTS-lip

Group		GTS-lip	Suc-GTS-lip
EE (%)	GA	88.56 ± 0.17	86.15 ± 0.46
	TSN	80.63 ± 0.91	81.70 ± 1.32
	Sal B	96.03 ± 0.28	91.05 ± 0.59
DL (%)		13.48 ± 0.69	19.40 ± 0.30
Size (nm)		120.5 ± 1.62	128.7 ± 2.10
Zeta (mV)		11.6 ± 0.35	15.5 ± 0.76
IR		/	96.58 ± 0.49

3.2 Accumlative release of TSN and GA in lip and solution in vitro

Table 5
Accumlative release of TSN and GA in lip and solution in vitro(n = 3)

Time(h)	Accumlative release (%)			
	TSN-lip	TSN-solution	GA-lip	GA-solution
1	0.52 ± 1.18	0.57 ± 2.10	0.71 ± 2.10	0.78 ± 2.27
2	2.21 ± 0.25	2.98 ± 1.36	1.81 ± 1.36	2.44 ± 2.29
4	3.03 ± 1.64	5.07 ± 3.15	3.63 ± 1.47	6.06 ± 2.16
8	8.62 ± 1.17	12.01 ± 3.32	6.37 ± 1.32	9.61 ± 2.21
12	10.78 ± 1.61	16.39 ± 4.18	6.73 ± 1.27	10.23 ± 3.18
18	12.87 ± 1.60	26.35 ± 2.25	6.81 ± 2.29	12.94 ± 2.25
24	15.97 ± 1.37	35.14 ± 2.64	7.55 ± 1.16	17.37 ± 3.64
36	18.68 ± 1.75	39.23 ± 3.17	9.59 ± 2.21	19.18 ± 3.17

The results from Table 5 and Figs. 2–3 show that the two components in the liposome have a certain sustained release effect compared with the solution group, and the in vitro release curves of TSN and GA conform to the Higuchi equation, R1 = 0.9828, R2 = 0.9599.

3.3 Pharmacokinetic analysis

The mean plasma concentration-time profiles of Sal B, GA and TSN from the two formulations are presented in Fig. 4. Pharmacokinetic parameters of Sal B, TSN and GA were determined using non-compartmental analysis, and the pharmacokinetic parameters are summarized in Tables 6, 7 and 8, respectively.

Sal B, TSN, GA by intravenous admonition of GTS-lip and Suc-GTS-lip ($\bar{x} \pm s$, n = 5)

Table 6
Pharmacokinetic parameters of Sal B in mouse plasma of GTS-lip and Suc-GTS-lip ($\bar{x} \pm s$, n = 5).

Parameters	Sal B	
	GTS-lip	Suc-GTS-lip
$T_{1/2}$ (h)	2.73 ± 0.11	3.39 ± 1.36
AUC_{0-t} (μg·h·mL^{-1})	636.06 ± 27.73	550.39 ± 12.34**
$AUC_{0-\infty}$ (μg·h·mL^{-1})	816.14 ± 56.81	806.53 ± 53.25
MRT_{0-t}(h)	1.97 ± 0.09	1.85 ± 0.08*
$MRT_{0-\infty}$ (h)	3.66 ± 0.60	5.01 ± 0.91*
$T_{1/2}$, half-life period of SalB *in vivo*;		

AUC_{0-t}, area under the concentration- time curve from time zero to the last sampling time point;

$AUC_{0-\infty}$, area under the concentration- time curve from zero to the infinity;

MRT_{0-t}, the mean residence time of Sal B time zero to the last sampling time point;

$MRT_{0-\infty}$, the mean residence time of Sal B time zero to the infinity;

Comparison between the two groups, **P < 0.01.

Comparison between the two groups, *P < 0.05.

Table 7

Pharmacokinetic parameters of TSN in mouse plasma of GTS-lip and Suc-GTS-lip ($\bar{x} \pm s$, n = 5).

Parameters	TSN	
	GTS-lip	Suc-GTS-lip
$T_{1/2}$ (h)	0.06 ± 0.02	0.05 ± 0.01
AUC_{0-t} (μg·h·mL^{-1})	1.08 ± 0.72	0.65 ± 0.04**
$AUC_{0-\infty}$ (μg·h·mL^{-1})	1.12 ± 0.72	0.65 ± 0.04**
MRT_{0-t} (h)	0.05 ± 0.01	0.13 ± 0.03**
$MRT_{0-\infty}$ (h)	0.06 ± 0.01	0.13 ± 0.03**
$T_{1/2}$, half-life period of TSN $_{in\ vivo}$;		
AUC_{0-t}, area under the concentration- time curve from time zero to the last sampling time point;		
$AUC_{0-\infty}$, area under the concentration- time curve from zero to the infinity;		
MRT_{0-t}, the mean residence time of TSN time zero to the last sampling time point;		
$MRT_{0-\infty}$, the mean residence time of TSN time zero to the infinity.		

Comparison between the two groups, **P < 0.01.

Comparison between the two groups, *P < 0.05.

Table 8
Pharmacokinetic parameters of GA in mouse plasma of GTS-lip and Suc-GTS-lip ($\bar{x} \pm s$, n = 5).

Parameters	GA	
	GTS-lip	Suc-GTS-lip
$T_{1/2}$ (h)	0.21 ± 0.01	1.00 ± 0.50*
AUC_{0-t} (μg·h·mL^{-1})	43.64 ± 3.10	96.21 ± 3.75**
$AUC_{0-\infty}$ (μg·h·mL^{-1})	44.06 ± 3.29	98.50 ± 3.70**
MRT_{0-t} (h)	0.50 ± 0.10	0.52 ± 0.07
$MRT_{0-\infty}$ (h)	0.53 ± 0.12	0.58 ± 0.09
$T_{1/2}$, half-life period of GA in vivo;		

AUC_{0-t}, area under the concentration- time curve from time zero to the last sampling time point;

$AUC_{0-\infty}$, area under the concentration- time curve from zero to the infinity;

MRT_{0-t}, the mean residence time of GA time zero to the last sampling time point;

$MRT_{0-\infty}$, the mean residence time of GA time zero to the infinity.

Comparison between the two groups, $^{**}P < 0.01$.

Comparison between the two groups, $^{*}P < 0.05$.

As shown in Table 6 to Table 8, the Sal B and TSN AUC0-t were higher in plasma administered with GTS-lip than those administered with Suc-GTS-lip, which infered more Sal B and TSN were distributed in tissue with the ligand's incorporation.

It has been reported that Sal B was unstable neither in whole blood nor plasma, and it is more unstable in whole blood than in plasma(Zhang et al.2013). Add some hydrochloric acid or formic acid to control pH of samples in the rage of 2.5-5 could inhibit SalB' decomposing. In this research, therefore, plasma samples were separated quickly and added formic acid-water solution to protect Sal B from degradation before cryopreservation.

Sal B is a compound with highly plasma protein binding rate, with the participation of ligand, liposomes' integrality was improved to protect Sal B from combining with plasma proteins and distribute in tissue better. The GA AUC0-t was increased from 43.64 ± 3.10μg•h•mL-1 to 96.21 ± 3.75μg•h•mL-1 after mix with

the ligand. It might because the ligand is just embedding in outer lipid physically, instead of synthesis on phospholipid chemically. And part of GA in plasma might be a breakdown product of the 18-GA-Suc.

3.4 Tissue distribution of liposomal components

The distribution of Sal B, TSN and GA in mouse organs at different time points after administration of the two formulations are shown in Figs. 5 to 7.

As figures showed, Sal B's distribution in liver was significantly higher administrated with Suc-GTS-lip than GTS-lip group, which illustrate that Sal B was embedded in water phase stably and was taken by hepatocyte with the help of 18-GA-Suc, the hepatocyte- targeting carrier. TSN could not be detected in liver after 1 h in the group which was administrated with Suc-GTS-lip. On the contrary, 6 h after administrated the TSN could still be detected in mouse's liver of GTS-lip group. Which infer that in Suc-GTS-lip, TSN could be transferred in liver with hepatocyte- targeting carrier quickly and be metabolized. Compared with GTS-lip, the distribution of GA in liver was decreased with administration of Suc-GTS-lip. It might because the GA, which was generated from 18-GA-Suc's breakdown, had the competitive inhibition in drug's combination with hepatocyte.

3.5 Evaluation of liver targeting ability of GTS-lip and Suc-GTS-lip

The liver targeting abilities of GTS-lip and Suc-GTS-lip were evaluated by the relative rate of uptake (Re), ratio of the maximum peak concentration (Ce) and targeting efficiency (Te). Results are shown in Tables 9 and 10. Calculation formulas are as follows:

$Re = AUC_{Suc\text{-}GTS\text{-}lip} / AUC_{GTS\text{-}lip}$

$Ce = (C_{max})_{Suc\text{-}GTS\text{-}lip} / (C_{max})_{GTS\text{-}lip}$

$Te = AUC_{liver} / AUC_{other\ organs}$

$AUC_{Suc\text{-}GTS\text{-}lip}$, area under the concentration-time curve from time zero to the last sampling time point after administration of Suc-GTS-lip;

$AUC_{GTS-lip}$, area under the concentration-time curve from time zero to the last sampling time point after administration of GTS-lip;

$(C_{max})_{Suc-GTS-lip}$, maximum concentration of drug in liver after administration of Suc-GTS-lip;

$(C_{max})_{GTS-lip}$, maximum concentration of drug in liver after administration of GTS-lip;

AUC_{liver}, area under the concentration-time curve from time zero to the last sampling time point after administration of Suc-GTS-lip in liver;

$AUC_{other\ organs}$, area under the concentration-time curve from time zero to the last sampling time point after administration of Suc-GTS-lip in other organs.

Table 9 Comparison of AUC and C_{max} between Suc-GTS-lip and GTS-lip in liver (n = 5)

Parameters	Sal B	TSN	GA
$AUC_{Suc-GTS-lip}$	$26.03 \pm 4.66^{**}$	$0.84 \pm 0.10^{**}$	24.54 ± 2.27
$AUC_{GTS-lip}$	2.55 ± 0.63	1.44 ± 0.25	26.63 ± 1.15
Re	10.21	0.58	0.92
$(C_{max})_{Suc-GTS-lip}$	$22.40 \pm 3.15^{**}$	$1.97 \pm 0.19^{*}$	18.16 ± 0.95
$(C_{max})_{GTS-lip}$	5.05 ± 0.76	2.29 ± 0.75	19.40 ± 0.36
Ce	4.44	0.86	0.93
Significantly different from GTS-lip group, $^{**}P < 0.01$, $^{*}P < 0.05$.			

Table 10 Comparison of targeting efficiency between liver and other tissues in Suc-GTS-lip (n = 5)

Te	liver	heart	spleen	lung	kidney
$Te_{Sal\ B}$	1	NA	1.35	1.95	4.70
Te_{TSN}	1	0.11	0.07	NA	0.12
Te_{GA}	1	NA	0.47	1.32	1.56
NA: Drugs were not applicable.					

As shown in Table 10, compared with the group which was treated with GTS-lip, the AUC and Cmaxin liver were 10.21 and 4.44 times in group which was administrated with Suc-GTS-lip respectively, which proved that the ligand, 18-GA-Suc, could improve distribution of drugs to liver which were embedded in liposome's inter water phase.

The TSN and GA were wrapped in outer phospholipid bilayer, get into body quickly along with liposomes and widely distributed in various tissues. TSN was metabolized rapidly in liver because its low drug-loading rate, which makes its AUC in liver lower than in other organs significantly. In the other hand, Sal B, which was embedded in inter water phase, could enter in liver along with liposomes under liver targeting ligand's help. In spite of the Sal B could not be detected in heart, the AUC SalB in liver was 1.35, 1.95, 4.70 times compared with AUCSalB in spleen, lung and kidney respectively, which infer that it is easier to get into liver for drugs in liposomes' inter water phase.

3.6 Fluorescent imaging of liposome distribution

3.6.1In vivo imaging of mice

Suc-GTS-lip was labeled with a lipophilic near-infrared fluorescent dye (DiR-iodide) and was injected via tail vein into KM mice. After intravenous injection, the mice were photographed at different time points using the fluorescence analyzer. The experimental animals were sacrificed after photography, and heart, liver, spleen, lungs, and kidneys were also photographed using the fluorescence analyzer. We finally compared the organ distributions of the two preparations at each time point. The results are shown in Fig. 8.

As Fig. 8 shows, liposomes distributed all over the body along with blood after administrated Suc-GTS-lip 10 min. Cause there are no furs at head and four limbs, the fluorescence intensity is stronger in these location. And the fluorescence signal could already be detected in chest and stomach. In 30 min, the liposomes had a trend to gather in chest and stomch. After 60 min, the fluorescent material, DiR-iodide, was metabolized gradually and fluorescence intensity was weaker and weaker all over the body.

It was found that tween-80 can't dissolve enough DiR to achieve the same fluorescence intensity in Suc-GTS-lip as. So the control group in this part can't be comparable. But in control group, it was observed that after administrated DiR solution, the fluorescence intensity was strongest in lung, which could conclude that Suc-GTS-lip had ability to change drugs' distribution.

3.6.2Ex vivo imaging of mouse organs

The imaged mouse organs are shown in Fig. 9. The fluorescence intensity was strongest in the liver at 30 minutes after administration of liposomes. After 60 min, the fluorescence signal had faded.

The results of in vitro mice organs imaging were shown in Fig. 6. The fluorescence intensity was strongest in liver after administrated liposomes 30 min. After 60 min, fluorescence signal was faded. And the fluorescence intensity was stronger in liver than any other organs at each time point.

3.7 Effects of SUco-GTS-LIP on proliferation inhibition and apoptosis of hepatic stellate cells

From Table 11, we know that the blank liposome group has no proliferation inhibitory effect on HSC, while the inhibitory effect of group Suc-GTS-lip on HSC increased with the increase of drug concentration. And in 24h, there is a certain dose-effect relationship. So we selected three drug concentrations (divided into high, medium and low dose groups) of Suc-GTS-lip for the next step to reveal the apoptotic effect of Suc-GTS-lip induced by HSC.

Table 11
In vitro inhibition of Suc-GTS-lip against HSC (x ± s, n = 6)

Groups	The proliferation inhibition rates	
	24h	48h
Suc-GTS-lip1	77.08 ± 1.95	81.78 ± 1.26
Suc-GTS-lip2	77.32 ± 1.67	83.04 ± 1.09
Suc-GTS-lip3	44.13 ± 4.22	83.22 ± 1.13
Suc-GTS-lip4	18.97 ± 4.67	40.65 ± 3.39
Suc-GTS-lip5	12.74 ± 5.22	7.21 ± 3.51
Blank-lip	2.90 ± 4.43	4.52 ± 5.86
Healthy Cells(Control Group)	——	——

The Fig. 9 shows that compared with the blank control group, Suc-GTS-lip treatment group can induce HSC apoptosis in varying degrees, and the greater the concentration, the more obvious the apoptosis. The main manifestation was that the stellate tentacles gradually atrophied, cell shrunk and cell gap increased.

From Table 12 and Fig. 10, the rate of apoptosis in normal HSC group was 4.20 + 1.04%.Compared with the blank control group, the Suc-GTS-lip in the three groups all played roles in inducing the apoptosis of HSC. The apoptotic rates of three groups of high, medium and low doses were 75.23 ± 2.56%,27.60 ± 0.95% and 20.77 ± 3.97%. It can be seen that the apoptosis rate of the middle and low dose groups was very close, while the apoptosis of the high dose group was obvious.

Table 12
Apoptosis rate of HSCs by flow cytometry (± s, n = 3)

Groups	Apoptosis rate(%)
Suc-GTS-lip(High-dose)	75.23 ± 2.56
Suc-GTS-lip(Medium-dose)	27.60 ± 0.95
Suc-GTS-lip(Low-dose)	20.77 ± 3.97
Healthy Cells(Control Group)	4.20 ± 1.04

From Fig. 11, we can see that the mRNA bands of MMP-1, TIMP-1, TIMP-2, Collagen-I and Collagen- III in hepatic stellate cells were clearly visible and could be used for quantitative gray scale analysis.

From Table 13 and Fig. 12 and the results of RT-PCR test also showed that the expression of MMP-1 in each group increased significantly compared with the control group, after the intervention of Suc-GTS-lip in the high, medium and low dose groups 24h. Among them, the *P* of high and middle dose group was

less than 0.001, the *P* of low dose group was less than 0.01. The expression of TIMP-1 and TIMP-2 in each drug group decreased significantly, among which the *P* of high and middle dose group was less than 0.001, the *P* of low dose group was less than 0.01. In low dose group, the expression of TIMP-1 was decreased that the *P* was less than 0.05, and the expression of TIMP-2 ($P < 0.01$) was similar to that in middle dose group.

Table 13
Effects of Suc-GTS-lip on mRNA expression of MMP-1, TIMP-1 and TIMP-2

Groups	MMP-1/Beta-actin	TIMP-1/Beta-actin	TIMP-2/Beta-actin
High-dose	0.39 ± 0.02***	0.31 ± 0.01***	0.29 ± 0.05***
Medium-dose	0.35 ± 0.01***	0.40 ± 0.01**	0.36 ± 0.01**
Low-dose	0.31 ± 0.02**	0.42 ± 0.04*	0.36 ± 0.01**
Control	0.21 ± 0.05	0.50 ± 0.04	0.48 ± 0.06
Note: Compared with control group: *P□0.05□**P□0.01□***P□0.001			

From Table 14 and Fig. 13and the results of RT-PCR test also showed that mRNA expression of Collagen-□and Collagen-□ in each group decreased significantly compared with the control group, after the intervention of Suc-GTS-lip in the high, medium and low dose groups 24h. Among them, the *P* of high and middle dose group was less than 0.001, the *P* of low dose group was less than 0.05.

Table 14
Effects of Suc-GTS-lip on mRNA expression of Collagen-□ and Collagen-□

Groups	Collagen-□/ Beta-actin	Collagen-□/ Beta-actin
High-dose	0.40 ± 0.01***	0.40 ± 0.04***
Medium-dose	0.43 ± 0.02***	0.42 ± 0.02***
Low-dose	0.51 ± 0.01*	0.49 ± 0.01*
Control	0.55 ± 0.04	0.55 ± 0.02
Note: Compared with control group: *P□0.05□**P□0.01□***P□0.001		

4 Conclusions And Discussions

It has been reported that Sal B is unstable in plasma, and moreso in whole blood (Zhang et al.2013). Addition of hydrochloric acid or formic acid to control the pH of samples within the range of 2.5-5 could inhibit the decomposition of Sal B. In this research, therefore, plasma samples were separated quickly and supplemented with a formic acid-water solution to protect Sal B from degradation before cryopreservation.

The fluorescence intensity is stronger at the head and forelimb areas due to the lack of fur in these locations. Moreover, the fluorescence signal could already be detected in the chest and stomach. Within 30 min, the liposomes tended to accumulate in the chest and stomach. After 60 min, the fluorescent material, DiR-iodide, was metabolized gradually and resulted in increasingly weaker fluorescence intensity throughout the body. Since the presence of fur influences the fluorescence signal, we are considering using nude mice to verify these results.

In the experiment, it was found that the DiR dye had strong fat solubility. When the DiR solution control group was prepared, the same fluorescence intensity as that of the DiR contained in the Suc-GTS-lip could not be obtained by using Tween 80 as a solubilizing agent, and thus it was not comparable. However, it can be seen from the preliminary experiments that the distribution of the DiR solution control group in the mouse is the strongest fluorescence intensity in the lung, so it can be concluded that Suc-GTS-lip has the effect of changing the drug distribution properties.

It can be seen from the results of small animal in vivo imaging experiments that the distribution of Suc-GTS-lip in the liver is higher than that of other organs, showing a certain liver targeting.

The drug delivery system Suc-GTS-lip will be uptaked through the interreaction between 18-GA-Suc and GA acceptor. However, the drug GA also uptake through GA acceptor. Will they affect each other? In the screening dose trials, it was shown that the drug content in the liver increased with increasing doses. This indicates to some extent that the GA receptor in the liver is not saturated when the therapeutic amount is administered, and the drug GA and the receptor 18-GA-Suc do not compete with the GA receptor of the liver.

MTT colorimetric assay was used to determine the cytotoxicity and growth inhibition of the cells(Kumar P et al.2018), which could be used as the first choice for in vitro drug screening.In this study, the MTT colorimetric method was used to screen the inhibitory effect of SUC-GTS-LIP on the proliferation of hepatic stellate cells.Three concentrations of liposomes with inhibition rates higher than 50%, 20–50% and lower than 20% were selected for follow-up experiments to observe the correlation between MTT assay and flow cytometry detection of apoptosis.

In this experiment, the sum of the percentage of apoptosis in the upper right quadrant and the lower right quadrant was taken as the total apoptosis rate for comparison. However, it can be seen from Fig. 10 that the late apoptosis rate of cells in each drug administration group was significantly higher than the early apoptosis rate, and it was speculated that the reason might be that the drug administration time of 24h was too long, and cells gradually developed from early apoptosis to late apoptosis.

Activated hepatic stellate cell (HSC) is the core of hepatic fibrosis, and its apoptosis is the key to the reversal of hepatic fibrosis.Recent studies have shown that the main pathological changes of hepatic fibrosis are the deposition of extracellular matrix (ECM), of which Collagen- □ and Collagen- □ are the main components. The synthesis rate of type □ and □ collagen is accelerated in liver fibrosis, accounting for more than 95% of the total liver collagen (He et al.

2017), which is closely related to the development degree of liver fibrosis. MMPs and TIMPs are the main enzymes regulating extracellular matrix, and matrix metalloproteinase MMPs is the main enzyme responsible for collagen degradation in liver, in which MMP-1 plays an important role in the degradation of type Ⅰ and Ⅲ collagen, the main components of extracellular matrix in fibrosis liver(Yang et al.2000). Matrix metalloproteinase inhibitors TIMPs include TIMP-1, 2, 3, and 4, TIMP-1 and TIMP-2 are are mainly expressed in the liver(Huang et al.2022). Activated HSC can synthesize and release large amounts of TIMP-1 and TIMP-2, and inhibit matrix metalloproteinases from degrading collagen.Therefore, in this study, the mRNA levels of matrix metalloproteinases, matrix metalloproteinase inhibitors and collagen in HSC were measured by RT-PCR after 24h intervention of cultured hepatic stellate cells with actively targeted liposomes (CS-GTS-LIP). The results showed that the drug-carrying liposomes could increase the secretion of matrix metalloproteinase (MMP-1), decrease the secretion of matrix metalloproteinase inhibitors (TIMP-1 and TIMP-2), reduce the synthesis of type Ⅰ collagen and type Ⅲ collagen, and promote the degradation of extracellular matrix, thus alleviating the degree of liver fibrosis.

Declarations

Author contribution

WXL is responsible for the overall experimental design, technical guidance and financial support, GHD is responsible for the experimental design, experimental research and data analysis, LG provides the experimental platform and technical guidance. LJH and WYR provide solutions to problems arising during the experiment, LT contributed to writing and editing the manuscript.All authors read and approved the manuscript, and all data were generated in-house and that no paper mill was used.

Funding

This work was fnancially supported by the National Natural Science Foundation of China (grant number 81202928) and the Natural Science Foundation of Beijing Municipality (grant number 7123118).

Availability of data and materials Not applicable.

Ethical approval Not applicable.

Consent to participate Not applicable.

Consent for publication Not applicable.

Competing interests The authors declare no competing interests.

References

1. Cui YH, Wang XL and Yan ZG et al. (2003) Effects of Salianic-acid B for Cellular Oxidation and PCNA of Hepatic Stellate Cells in Rat. *Chinese Journal of Integrated Traditional and Western Medicine on*

Liver Diseases 4: 210-212.

2. Deng W,Chen Q,Gong ZJ(2021) Research progress in the treatment of liver fibrosis of different etiologies.Chinese Journal of Difficult and Complicated Cases 20(09):957-962
3. Fan F and Sun XF (2007) The research progress of the liver targeted drugs mediated by Galactose receptor. *J. Central South Pharm* 1: 62-65.
4. Hu YY, Liu P and Liu C et al. (1999) Influence of the Extract of Radix Salviae Miltiorrhizae on Heptic Fibrosis Induced by CCl4 and DMN in Rats. *Shanghai Journal of Traditional Chinese Medicine* 10: 7-10.Chinese.
5. He P,Wu YF,Yang HY,Cheng ML,Liang YD,Wang YP(2017)Effects of cannabinoid receptor-2 agonist AM1241 on expression of platelet-derived growth factors in hepatic tissue of mice with hepatic fibrosis.Chinese Journal of Hepatology 25(11):841-846
6. Huang Q,Yang Y,Zeng R,Yao ML,Sun Q(2022)Research progress of matrix metalloproteinase/matrix metalloproteinase hydrolase in regulating liver fibrosis and related drugs.Journal of Clinical Hepatology 1-6[2022-04-04].http://kns.cnki.net/kcms/detail/22.1108.R.20211221.1646.002.html
7. Ishida S, Sakiya Y and Ichikawa T et al. (1989) Pharmacokinetics of glycyrrhetic acid, a major metabolite of glycyrrhizin, in rats. *J. Chem. & Pharm Bull* 9: 2509-2513.
8. Kumar P, Nagarajan A, Uchil PD(2018)Analysis of Cell Viability by the MTT Assay. Cold Spring Harb Protoc Jun 1,2018(6). doi: 10.1101/pdb.prot095505. PMID: 29858338.
9. Kan Y,Yang Y(2019)The effect of salvianolic acid B on apoptosis of hepatic fibrosis cells was investigated based on Cleaved caspase-9.Chinese Pharmacological Bulletin 35(06):827-832
10. Lin JH, Wang XL and Wu Q et al. (2014) Development of Salvianolic acid B–Tanshinone II A–Glycyrrhetinic acid compound liposomes: Formulation optimization and its effects on proliferation of hepatic stellate cells. *J. Int. Journal of Pharm.* 462: 11-18.
11. Mao SJ, Huo SX and Jin H et al. (2003) Preparation of Liposomes Surface-modified with Glycyrrhetinic Acid Targeting to Hepatocytes. *J.China Journal of Chin. Materia Medica* 4: 328-331.
12. Tian J and Lv J (2006) The comparing study of the anti-hepatofibrosis effect of 18α- and 18 β-Glycyrrhizic acid in rats. Chin. *J. Journal of Modern Appl. Pharm* 2: 102-104.
13. Wang JY, Liu WT and Hu MY et al. (1997) Inhibitory effect of glycyrrhizic acid on expression of fibrolasts' I/III precollagen mRNA. *J. Chin. Journal of Dig* 1: 60-61.
14. Wang XL, Liu P and Cui YH et al. (2006) Inhibitory effect of salvianolic acid B on malondialdehyde-stimulated proliferation of rat hepatic stellate cells *in vitro*. *J. World Chin. Journal of Dig* 5: 476-480.
15. Wu C and Guo WY (2008) Liver Targeting Study on Glycyrrhetinic Acid Derivatives Modifying Norcantharidin Liposomes in Rats. *Journal of Liaoning Medical University* 6: 490-491.
16. Yang CQ,Hu GL,Tan DM,Zhang Z(2000)The relationship between the expression of MMP-1 TIMP-1 and the content of type collagen in experimental hepatic fibrosis.Journal of Clinical Hepatology (04):222-224

17. Yang Q and Zhao YY (2006) Targeting therapy of primary liver cancer. *J. The Journal of Practical Medicine* 4: 481-482.
18. Yuan Z, Huang W and Tian Q et al. (2015)Tian Si Polymer Materials Technology Development CO., Nankai University, assignee. Glycyrrhetinic acid-mediated nanoparticles of hepatic targeted drug delivery system, process for preparing the same and use thereof. A61K9/51, A61K47/36, A61K47/48.3 November 2015.
19. Ye ZR,Lin H,Liao HL9(2021)Research progress on the mechanism of circrnas in liver fibrosis.Medical Recapitulate 27(19):3767-3772
20. Zhang XJ, Huang X and Jiang ZZ et al.(2013) Stability Comparison of Salvianolic Acid B in Whole Blood and Plasma. *J. Pharm. And Clin. Res.* 3: 215-217.
21. Zhu SC,Zheng XM,Zhang Y,Liu L,Zhou ZX,Xu WR(2017)Experimental study of glycyrrhetinic acid derivatives against liver fibrosis.Chinese Traditional and Herbal Drugs 48(17):3554-3559

Figures

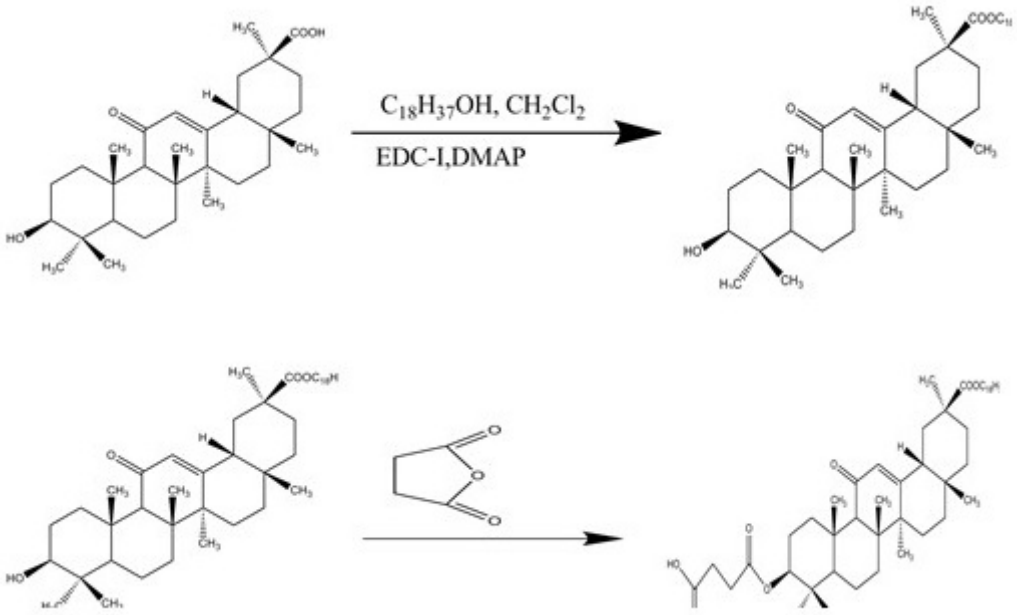

Figure 1

Synthetic process of 18-GA-Suc

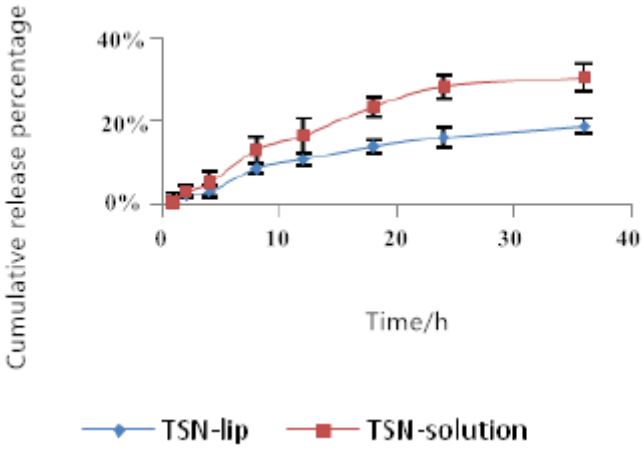

Figure 2

In vitro release curve of TSN

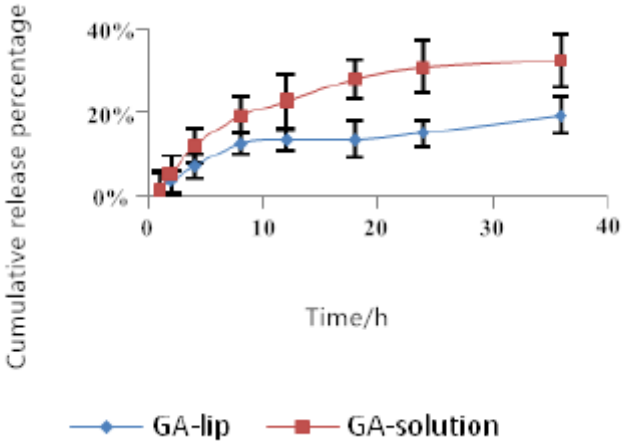

Figure 3

In vitro release curve of GA

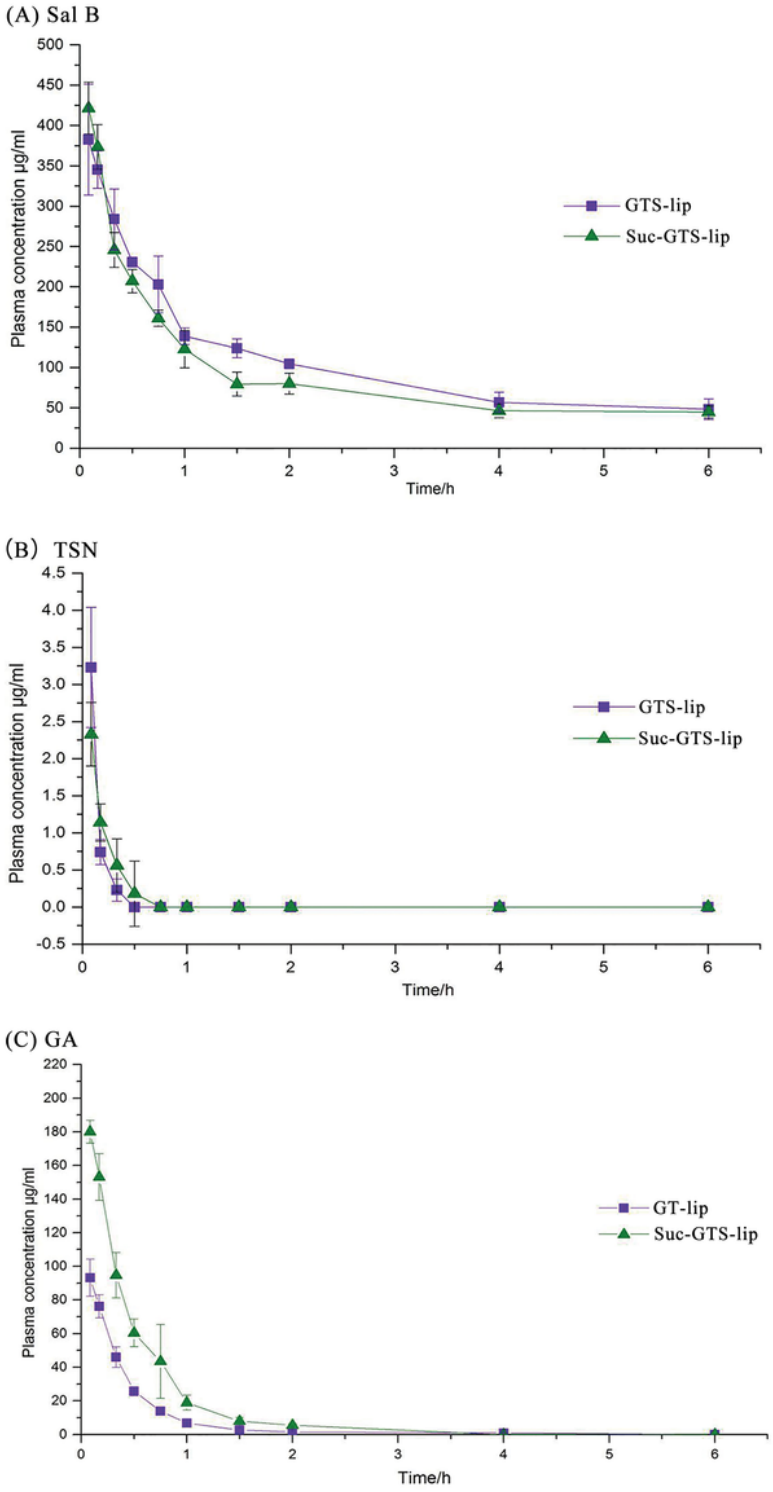

Figure 4

Mouse plasma concentration of Sal B, TSN, GA by intravenous admonition of GTS-lip and Suc-GTS-lip ($\bar{x}$ ±s, n=5)

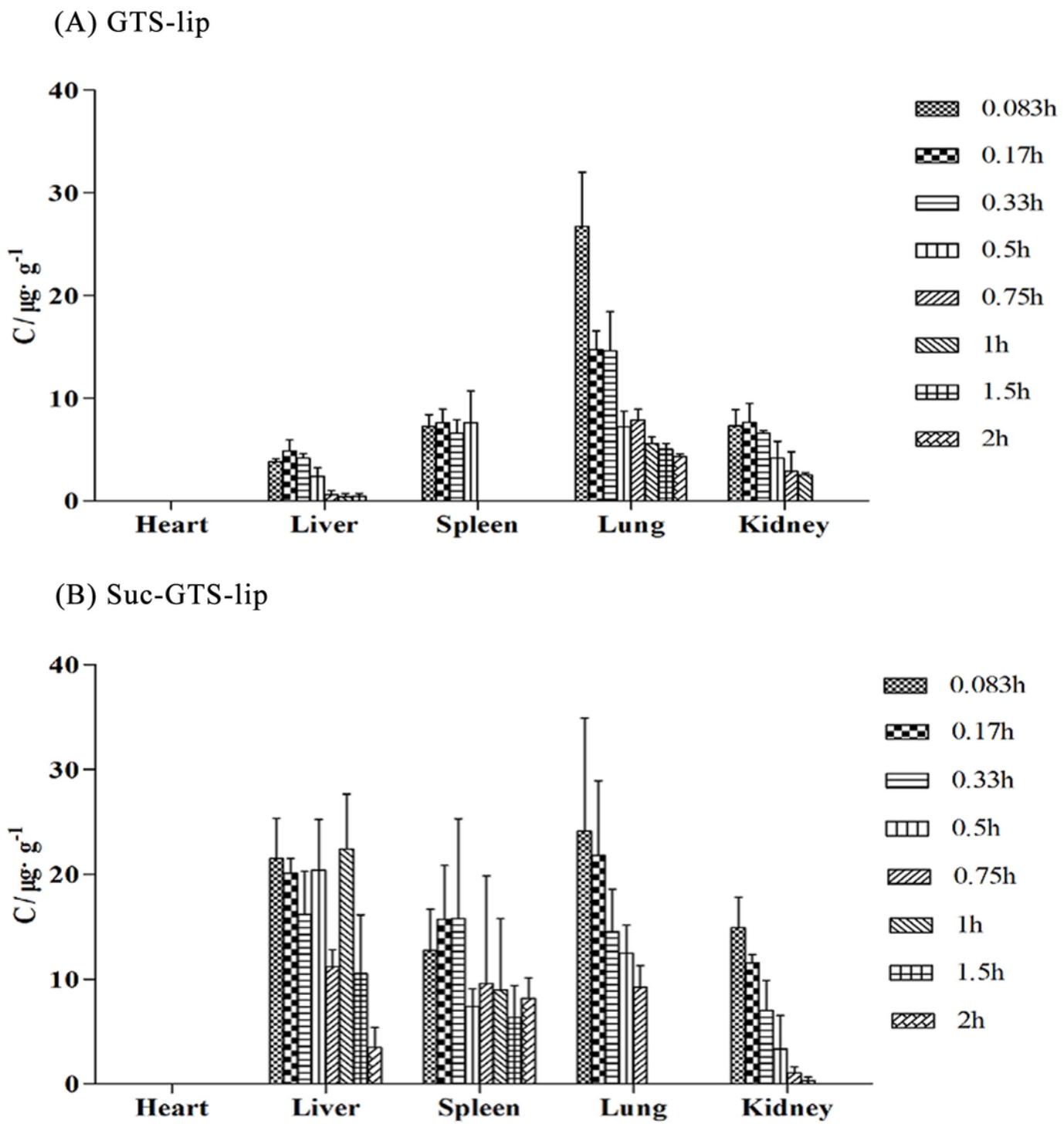

Figure 5

Distribution of Sal B in mice oragans at different time points after the intravenous administration of GTS-lip and Suc-GTS-lip ($\bar{x}$ ±s, n=5)

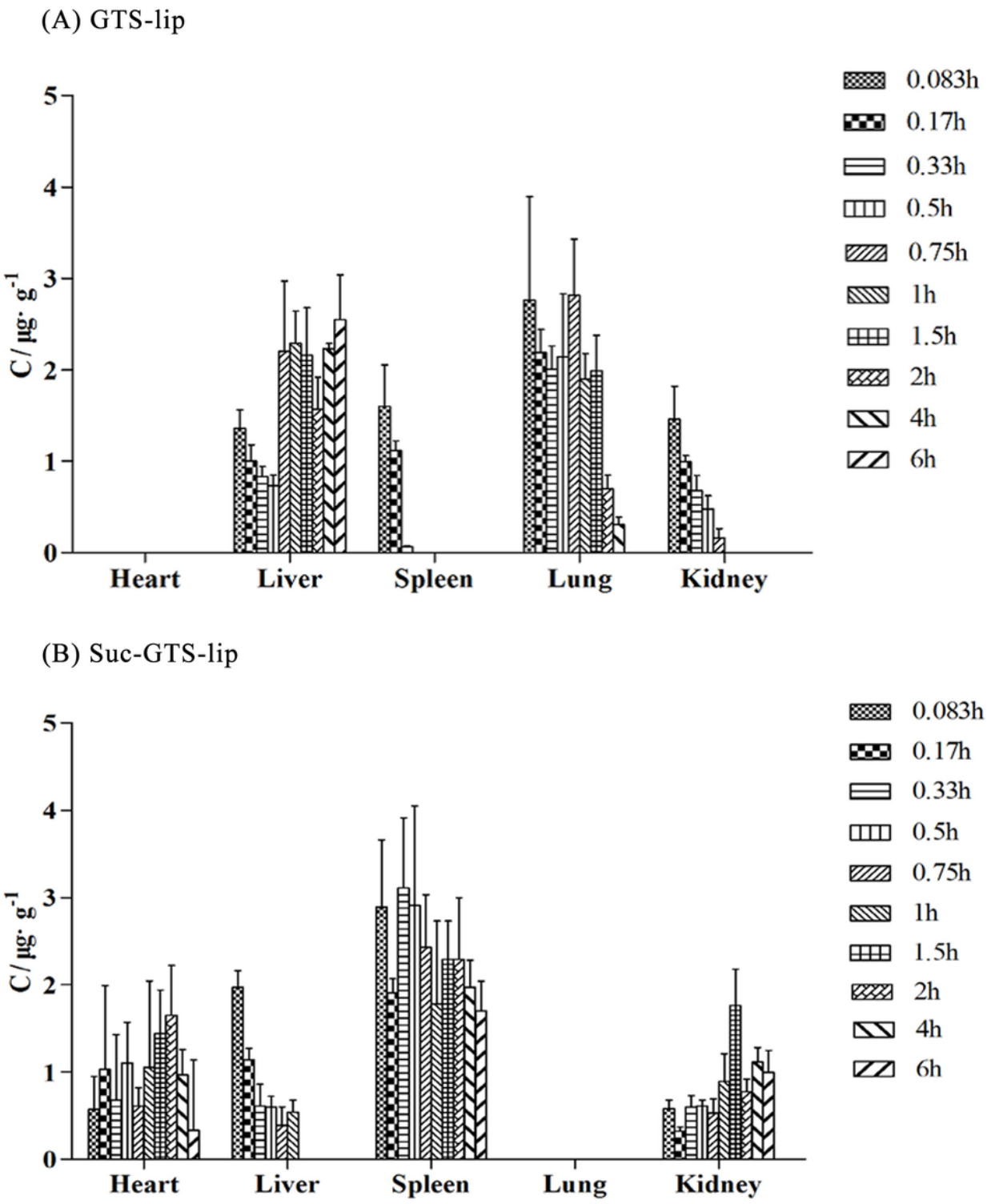

Figure 6

Distribution of TSN in mice oragans at different time points after the intravenous administration of GTS-lip and Suc-GTS-lip ($\bar{x}$ ±s, n=5)

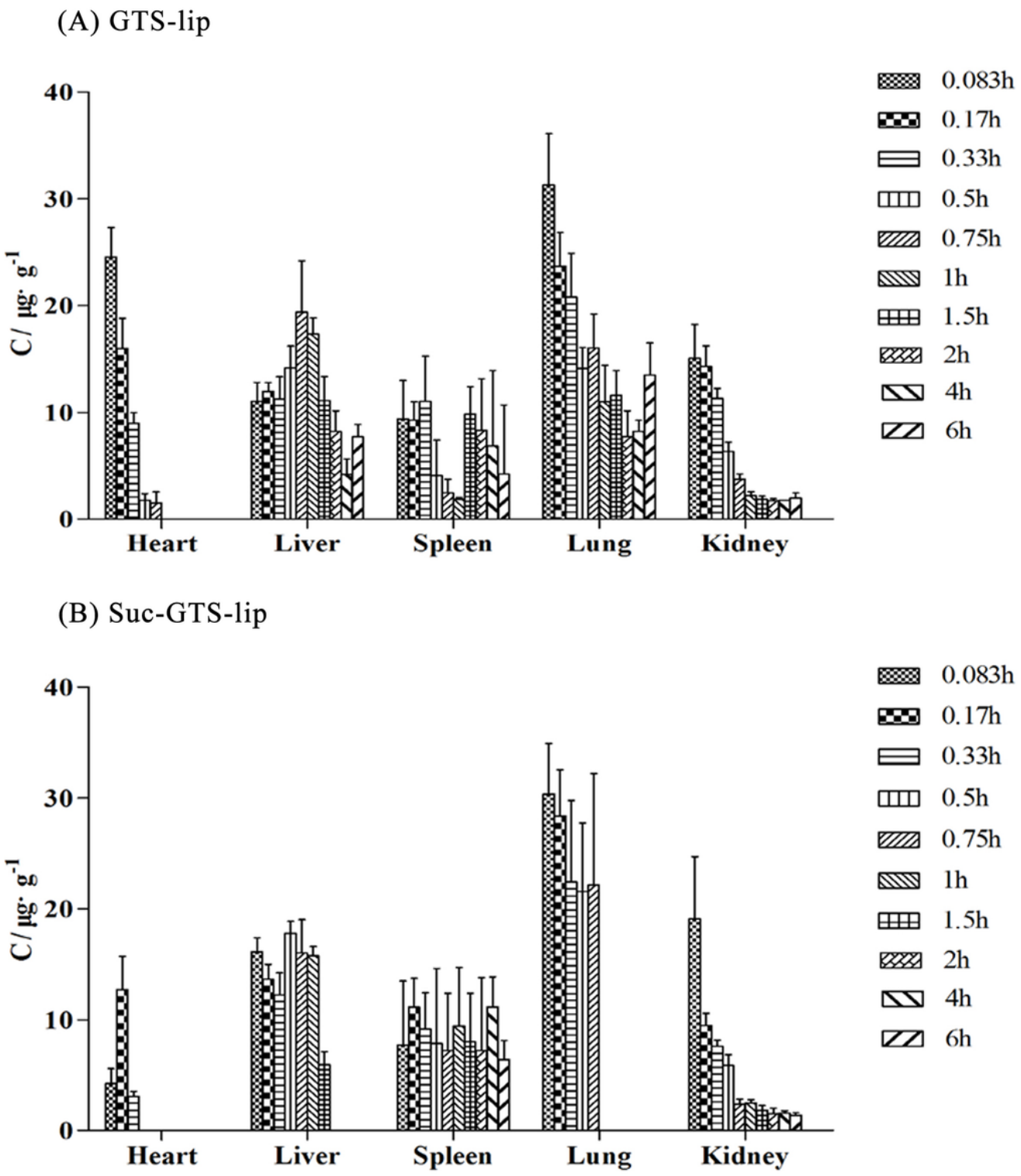

Figure 7

Distribution of GA in mice oragans at different time points after the intravenous administration of GTS-lip and Suc-GTS-lip ($\bar{x}$ ±s, n=5)

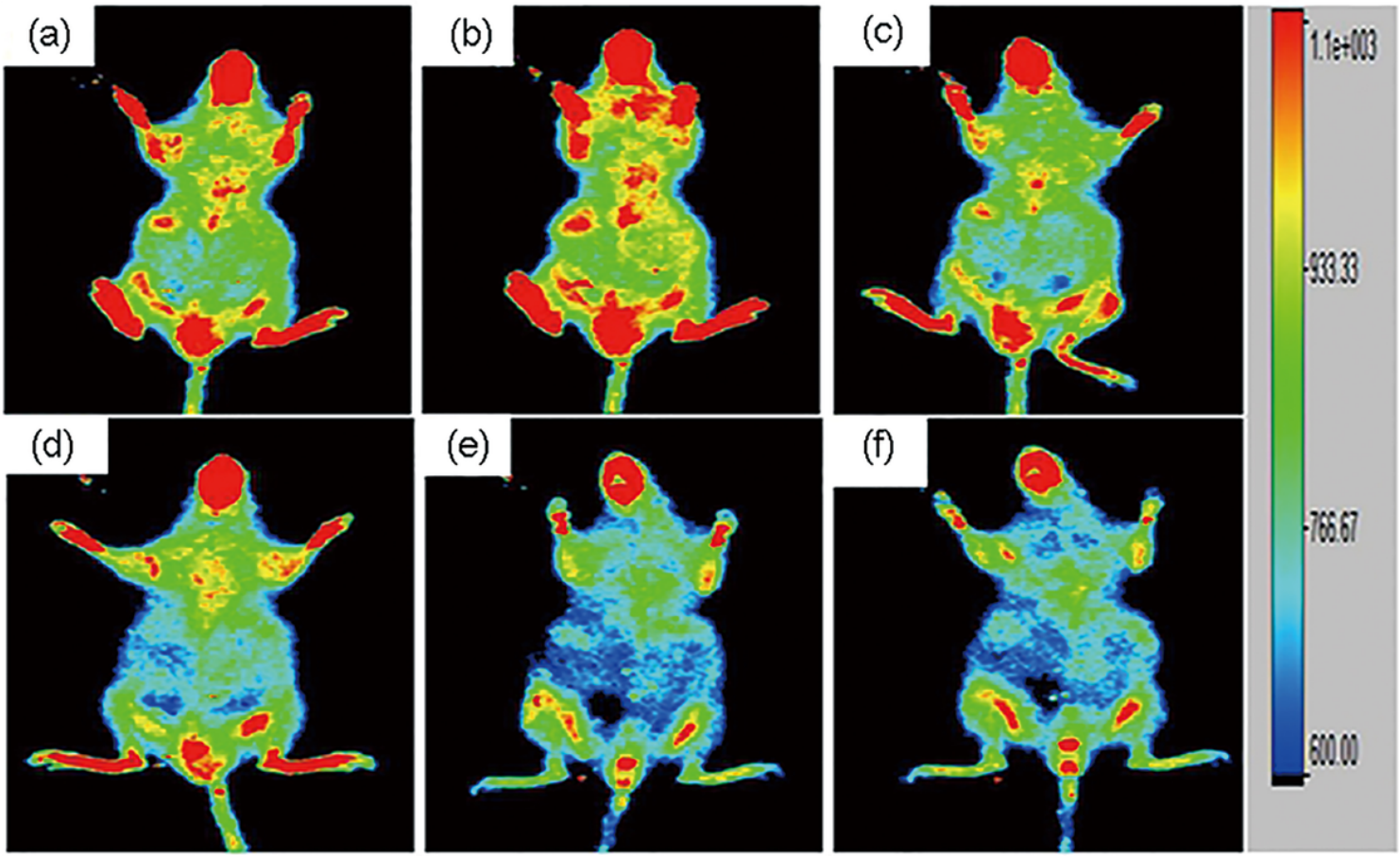

Figure 8

The results of fluorescent distribution in vivo

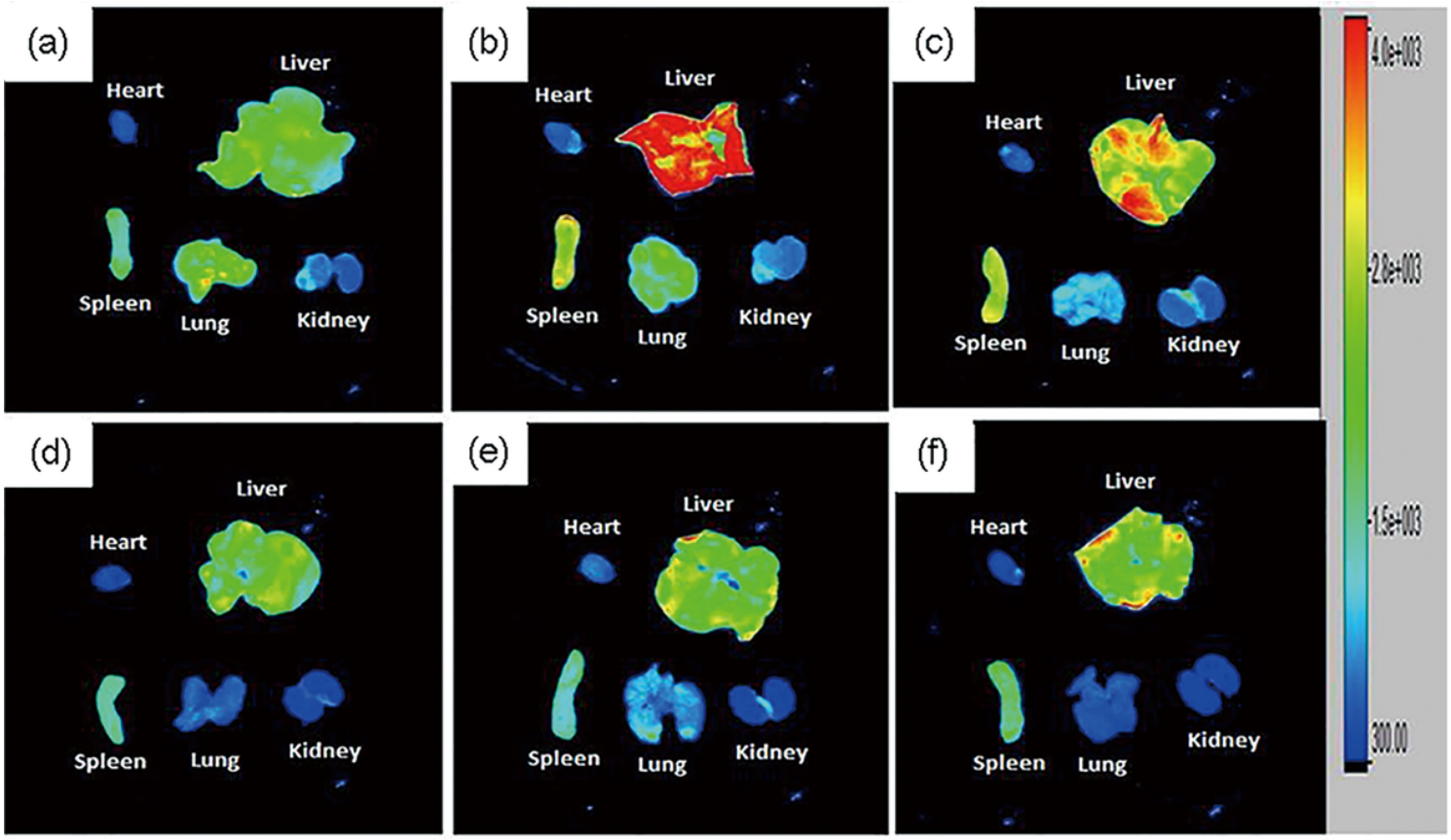

Figure 9

The results of fluorescent tissue distribution

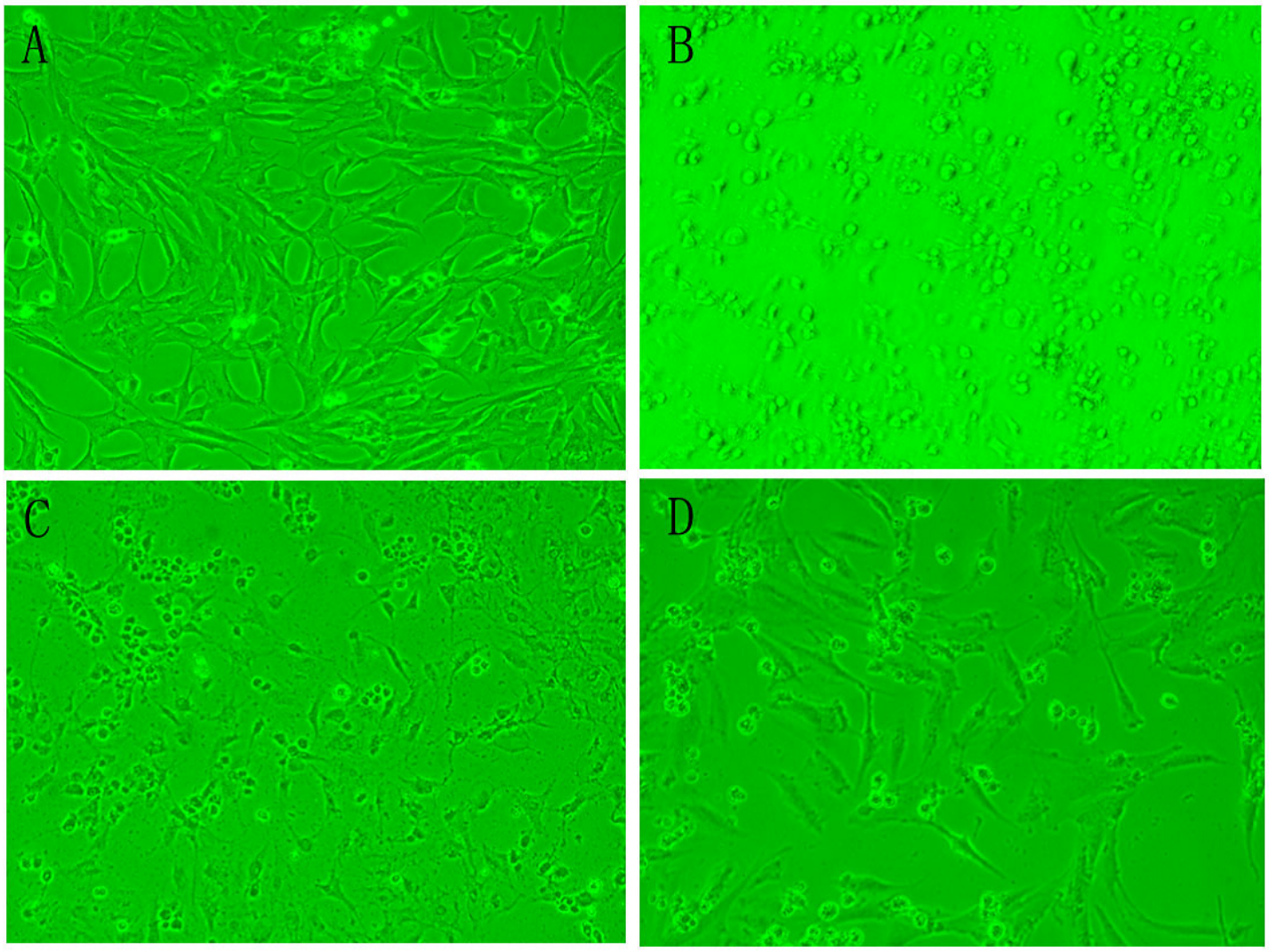

Figure 10

Figure 9 Phase-contrast images of cultured HSC after 24h incubation:

(A)Blank Control , (B)Suc-GTS-lip（High-dose）,

(C)Suc-GTS-lip（Medium-dose）, (D)Suc-GTS-lip（Low-dose）

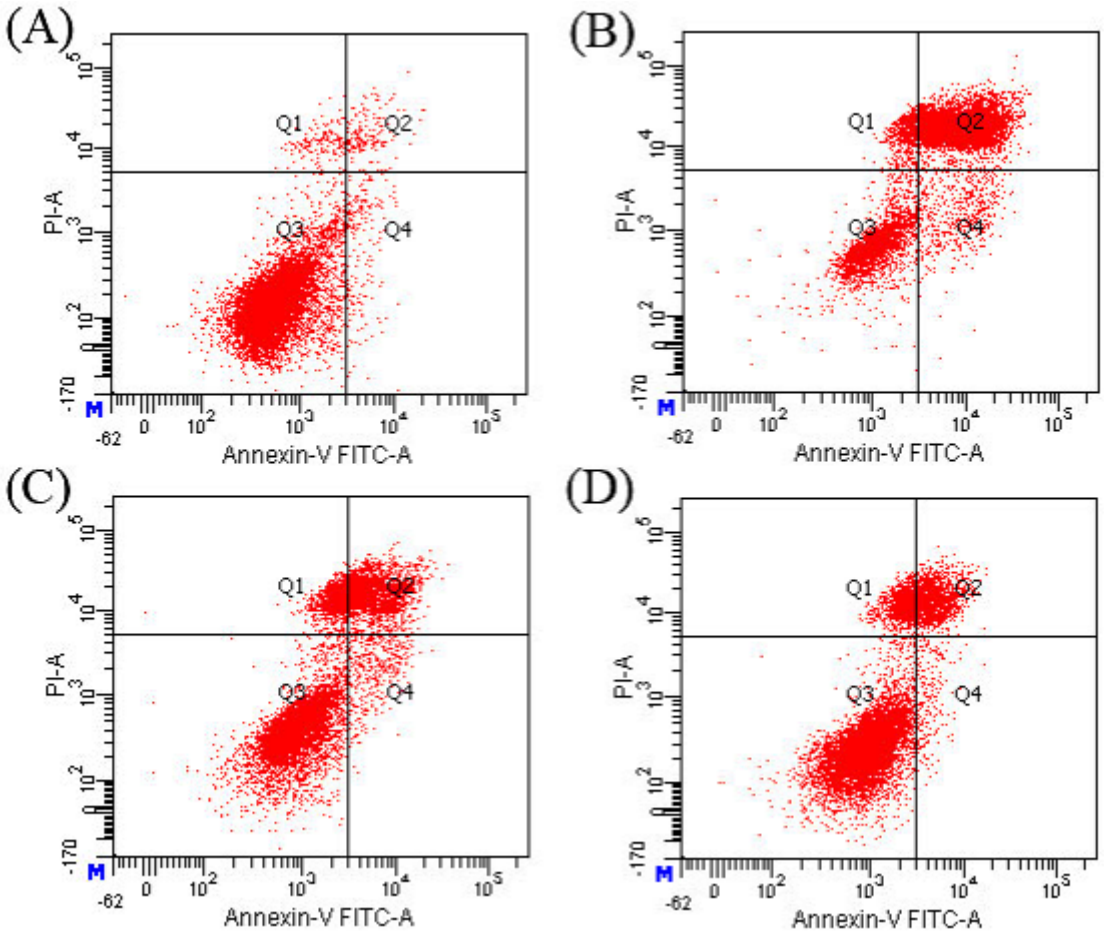

Figure 11

Figure 10 Determination of HSC apoptosis rate by flow cytometry (±s, n=3)

（A）Blank Control , (B) Suc-GTS-lip（High-dose）,

（C）Suc-GTS-lip（Medium-dose）,（D）Suc-GTS-lip（Low-dose）

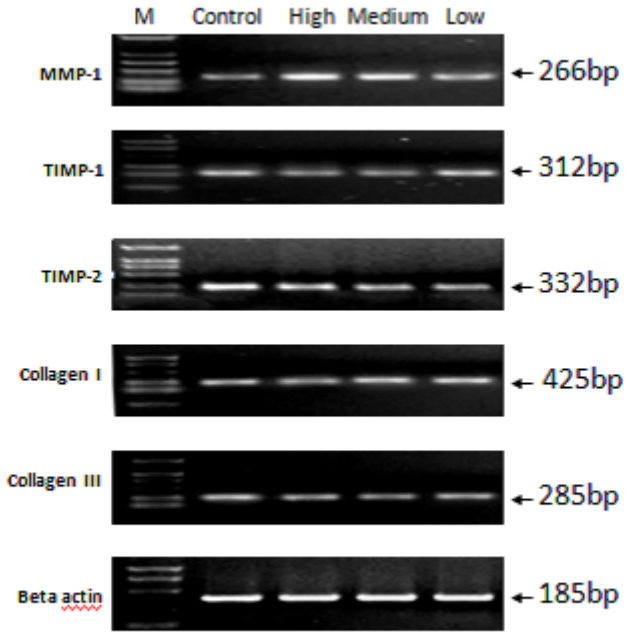

Figure 12

Gel electrophoresis of extracellular matrix mRNA in HSCs

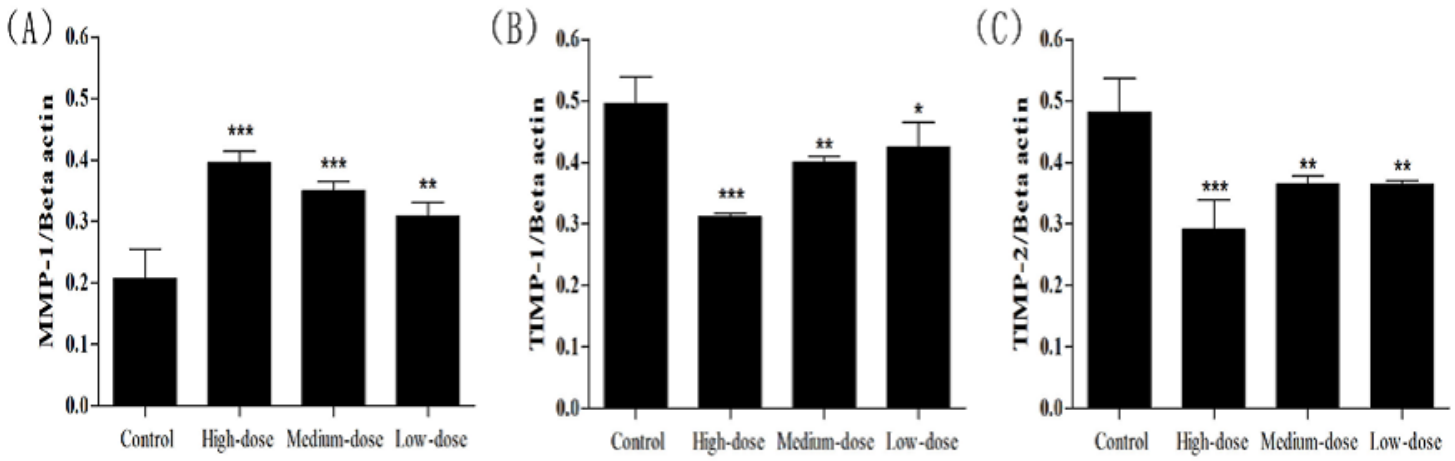

Figure 13

Figure 12 Effects of Suc-GTS-lip on mRNA expression of MMP-1(A), TIMP-1(B) and TIMP-2(C) in HSCs

Note: Compared with control group: *P□0.05□**P□0.01□***P□0.001

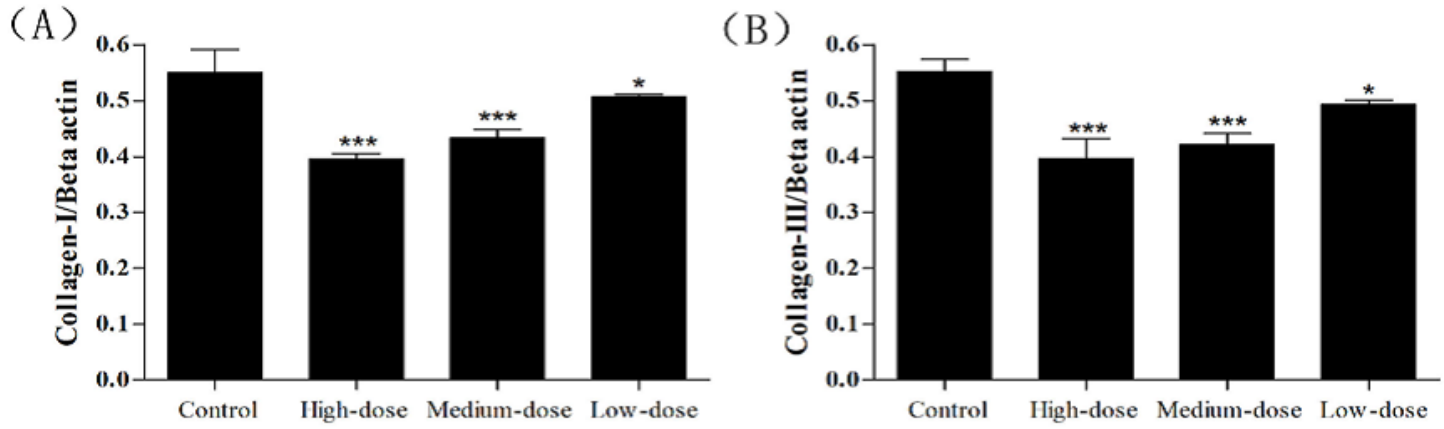

Figure 14

Figure13 Effects of Suc-GTS-lip on mRNA expression of Collagen-Ⅰ(A) and Collagen-Ⅲ(B) in HSCs

Note: Compared with control group: *P＜0.05，**P＜0.01，***P＜0.001